Nat Struct Mol Biol. Author manuscript; available in PMC 2011 December 07.

Published in final edited form as:
Nat Struct Mol Biol. 2011 February ; 18(2): 177–184. doi:10.1038/nsmb.1983.

Structural basis for the assembly of the SMRT/NCoR core transcriptional repression machinery

Jasmeen Oberoi[1,2,4], **Louise Fairall**[1,4], **Peter J. Watson**[1,4], **Ji-Chun Yang**[2], **Zsolt Czimmerer**[3], **Thorsten Kampmann**[1], **Benjamin T. Goult**[1], **Jacquie A. Greenwood**[1], **John T. Gooch**[2], **Bettina C. Kallenberger**[2], **Laszlo Nagy**[3], **David Neuhaus**[2], and **John W.R. Schwabe**[1,5]

[1]Henry Wellcome Laboratories of Structural Biology, Department of Biochemistry, University of Leicester, Lancaster Road, Leicester. LE1 9HN

[2]MRC-Laboratory of Molecular Biology, Hills Road, Cambridge. CB2 0QH

[3]Apoptosis and Genomics Research Group of the Hungarian Academy of Sciences, Department of Biochemistry and Molecular Biology, Life Sciences Building, Medical and Health Science Center, University of Debrecen, Debrecen, Egyetem ter 1. H-4032 Hungary

Abstract

Eukaryotic transcriptional repressors function by recruiting large co-regulatory complexes that target histone deacetylase enzymes to gene promoters/enhancers. Transcriptional repression complexes, assembled by the co-repressor NCoR, and its homologue SMRT, play critical roles in many processes including development and metabolic physiology. The core repression complex involves the recruitment of three proteins: HDAC3, GPS2 and TBL1 to a highly conserved repression domain within SMRT and NCoR. We have used a variety of structural and functional approaches to gain insight into the assembly, stoichiometry and biological role of this complex. We report the crystal structure of the tetrameric oligomerization domain of TBL1, which interacts with both SMRT and GPS2, and the NMR structure of the interface complex between GPS2 and SMRT. These structures, together with computational docking, mutagenesis and functional assays, reveal the assembly mechanism and stoichiometry of the co-repressor complex.

The regulated repression of transcription plays a key role in many biological processes. These include cell fate decisions during development and cellular differentiation, as well as the maintenance of homeostasis. SMRT and NCoR are large homologous co-repressor proteins that were identified through their role in transcriptional repression by many

[5]Corresponding author: john.schwabe@le.ac.uk.
[4]These authors should be considered co-first authors.

Author Contributions

The contributions of J.O., L.F. & P.W. were critical to the final manuscript and these authors should be considered co-first authors. J.O. (assisted by J.Gooch) performed most of the protein cloning, expression, purification and interaction mapping, although important preliminary experiments were performed by B.K. J.O. prepared the GPS2–SMRT complex for NMR structure determination which was carried out by J-C.Y. and D.N. Crystallizations were performed primarily by J.O., with some later trials by J.Greenwood and L.F. Crystal structure determinations were performed by L.F., J.O. and J.W.R.S. The interaction motifs in GPS2 and SMRT were identified by J.W.R.S. and tested by pull-down experiments by J.O. Fluorescence polarization, co-immunoprecipitation and co-transfection/ purification assays were performed by P.W. The two-hybrid assays, gel filtrations and NMR comparisons of WT and MT TBL1 were performed by P.W., Z.C. and B.G. *In silico* docking experiments were performed by T.K. The laboratories of L.N. and D.N. provided experimental expertise for transfection and NMR studies respectively. J.W.R.S. planned and supervised the project and prepared the manuscript with assistance from the other authors.

Accession Codes

1H, 13C and 15N NMR resonance assignments for the SMRT(167–207) – GPS2(53–90) complex have been deposited at the BioMagResBank under accession code 17271, and the coordinates have been deposited under the pdb accession code 215G. The TBL1 X-ray structures have been deposited with the PDB codes (2XTC, 2XTD & 2XTE).

different nuclear receptors, either in the absence of ligands, or when bound to synthetic antagonists [1]. SMRT and NCoR are also recruited by many other DNA-binding transcription factors including: BCL6, Kaiso, ETO, MEF2C, CNOT2 and CBF1 [2-8]. Hence SMRT and NCoR have important and general roles in mediating transcriptional repression. Indeed, mice lacking either SMRT or NCoR die during early embryogenesis due to multiple developmental failures [9,10]. In humans, SMRT and NCoR have been implicated in several leukemias, and the regulation of metabolism, life span and circadian physiology [3,11-15].

When purified from HeLa cell extracts, SMRT and NCoR are found within large assemblies with have an apparent molecular weight of 1.5-2MDa [16-18]. Various approaches have demonstrated that the SMRT/NCoR complexes are associated with multiple histone deacetylase enzymes suggesting a mechanism by which these proteins mediate transcriptional repression through the deacetylation and condensation of chromatin [19,20]. The relative importance of each of the various histone deacetylase enzymes has yet to be fully established; however, it has been demonstrated that HDAC3 recruitment to the complex is essential for repression by certain nuclear receptors as well as for normal circadian metabolic physiology [21,22]. Importantly, the enzymatic activity of HDAC3 is greatly enhanced through recruitment to the repressor complex through interaction with the SMRT DAD (Deacetylase Activation Domain)[23-25]. In addition to HDAC3, both SMRT and NCoR form stoichiometric complexes with the proteins GPS2 (also known as AMF1) and TBL1 (and/or its homologue TBLR1) [16,24,25]. GPS2 and TBL1 interact with the conserved core region of SMRT and NCoR, which has been characterized as repression domain 1 (RD1) [26]. GPS2 has been reported to interact with a number of transcriptional regulators including P53, LXR, RFX4_v3, papilloma virus proteins E2 and E6 as well as the DNA repair proteins hMSH4/5 [27-32]. In several of these cases it appears that GPS2 plays a role in transcriptional activation, but the role of GPS2 in both activation and repression complexes is poorly understood.

TBL1 is a WD40 repeat containing protein that is highly conserved from yeast to man and has been implicated in late-onset sensineural deafness [33]. In addition to TBL1, the closely related homologue, TBLR1, is also found associated with the co-repressor complexes. Both TBL1 and TBLR1 contain a strongly conserved N-terminal domain that has been suggested to contain LisH and F-box-like motifs. The F-box-like motif has been suggested to mediate interaction with the SCF ubiquitin ligase complex and with the E2 ubiquitin ligase UbcH5 [34]. The N-terminal domain of TBL1 has also been reported to mediate interactions with the tails of histones H2B and H4 [24,35,36]. Like GPS2, TBL1/TBLR1 are also thought to be involved in transcriptional activation. This may be explained by TBL1 acting as a co-regulator exchange factor [34].

We have used a variety of structural and functional approaches to gain insight into the assembly, stoichiometry and biological role of the core repression complex using human proteins expressed in bacteria and mammalian cells. We have closely mapped the regions required for formation of the SMRT–TBL1–GPS2 complex. The crystal structure of the minimal interaction region within TBL1 reveals a tetrameric, oligomerization domain, which mediates interaction with both SMRT and GPS2. We have identified a consensus motif in SMRT, NCoR and GPS2 that mediates interaction with this oligomerization domain of TBL1 and have modeled these interactions using mutation-guided docking protocols. We also report the NMR structure of the complex between SMRT and GPS2. This takes the form of a tight anti-parallel coiled coil. This coiled-coil is important since it means that a tight interaction with TBL1 will likely require both the SMRT and GPS2 co-regulator proteins. Together these structures and interaction studies reveal how TBL1 plays a central role in mediating the assembly of the transcriptional repression machinery.

Results

SMRT, TBL1 & GPS2 form a 3-way mutually interacting complex

Previous studies have shown that regions comprising residues 161-225 and 226-312 of SMRT are sufficient for interaction with GPS2(1-103) and TBL1(1-90) respectively [25]. We confirmed and refined these interaction regions using co-purification assays in which one component was tagged with either GST or His6 (Fig. 1). Figure 1a shows that a stoichiometric ternary complex can be readily co-purified and that this is the result of a three-way interaction. The figure shows that each component is also able to interact in binary complexes with the other components. Intriguingly SMRT(167-297) and GPS2(1-90) are both protected from proteolysis when in a complex with TBL1, but not when they interact with each other. This prompted us to map more closely the various interaction regions. Figure 1b shows that SMRT(167-207) is sufficient to interact with GPS2, but not TBL1. This interaction requires at the minimum, residues 53-90 of GPS2. The C-terminal fragment of SMRT(227-297) is sufficient to interact with the minimal domain of TBL1(1-71), but not GPS2. TBL1(1-71) in turn interacts with GPS2(1-60). This three-way interaction is schematized in figure 1c and these results suggest that TBL1 forms a single protease-resistant domain that interacts with both GPS2 and SMRT. These regions in SMRT and GPS2 are predicted to be natively unstructured linear motifs. Proteolysis observed in the co-purification assays (Fig. 1), as well as protease mapping (data not shown) supported the notion that SMRT and GPS2 become folded and resistant to proteolysis on interaction with TBL1. The mutually interacting regions in SMRT(167-207) and GPS2(53-90) are predicted to form a coiled coil.

To understand the assembly of the core repression complex we purified a number of single, binary and ternary complexes for structure determination. Many crystals of these complexes were obtained, but diffraction was limited to around 5Å. However we were able to determine the NMR structure of the complex between SMRT(167-207) and GPS2(53-90) and also the crystal structures of TBL1(1-90) and TBL1(1-71).

NMR structure of the SMRT–GPS2 complex

The structure of the minimal complex between SMRT(167-207) and GPS2(53-90) was determined using NMR spectroscopy. Figures 2a and b show an overlay of the ten structures with fewest NOE violations. The proteins interact through forming a coiled-coil structure. In this case the coiled-coil has an anti-parallel arrangement (Fig. 2c,d). This is somewhat unusual since the majority of coiled-coils observed in protein complexes adopt a parallel orientation [37]. However anti-parallel coiled coils are equally stereochemically favorable. The orientation of coiled-coils is specified, not in the non-polar amino acids involved in the interface core, but rather in the (mostly charged) residues located adjacent to the non polar core in positions a-g' & g-a' for parallel CCs a–a' & g–g' for antiparallel CCs - see figure 2. Figure 2d shows the favorable interactions that, in this case, uniquely specify an anti-parallel orientation (see also Supplementary Fig. 1a). Interestingly there are two pairs of acidic residues in apparent close proximity (GPS2:Glu58 – SMRT:Glu203 & GPS2:Glu82 – SMRT:Glu182). However, these apparently unfavorable interactions appear to be compensated by adjacent basic side chains.

An important consequence of the anti-parallel nature of the interaction between SMRT and GPS2 is that it positions the TBL1 interaction regions at one end of the coiled-coil.

Structures of TBL1-N-terminal domain

Two different diffraction quality crystal forms were obtained for different length constructs of the TBL1 N-terminal domain (TBL1-NTD). The longer construct (1-90) gave crystals of

spacegroup $P6_122$ that diffracted to 2.2Å. Crystals of the shorter construct (1-71, spacegroup $P3_212$) diffracted to 3.0Å.

The structure of the TBL1-NTD (1-90) was solved by molecular replacement using the dimeric two-helix LisH domain from Lis1 (pdbcode: 1uuj [38]). This equates to only 30% of the amino acids in the TBL1-NTD construct. Nevertheless a clear molecular replacement solution was obtained, but initially only limited electron density was apparent for the remainder of the structure, which was built during iterative rounds of refinement. The TBL1-NTD forms a tight dimer and these dimers further assemble to form a tetramer (Fig. 3a,b).

Dimer interface

The primary dimerization interface is formed from the conserved LisH motif and is shared in the related proteins Lis1 and FOP (Supplementary Fig. 1b) [38,39]. The LisH motif consists of two helices which come together to form anti-parallel four-helix bundle. In the interior of this bundle are the conserved non-polar amino acids which characterize the LisH motif. These include Val8, Val12, Tyr15, Leu16, Phe21, Phe28. There are also several conserved polar contacts at this interface. Of note is a hydrogen bond between the conserved sidechains of Tyr15 and Asn9'. Also Glu31 makes hydrogen bonds to the amides of Ser22', His23' and Ser24' and a charged interaction with the helix dipole. The dimerization interface in TBL1 is much more extensive than just the LisH motif. C-terminal to the LisH motif, there is an extended and irregular loop that wraps over the surface of the four-helix bundle and joins a third, more extended helix. This helix forms part of the dimer interface. The two helices cross over forming a symmetrical "X-shaped" structure that rests on the four-helix bundle. There are many non-polar interactions between the top of the four-helix bundle and the "X-shaped" structure. These include Ile3, Val8, Leu11, Tyr15, Ala48, Leu49, Ile50 and Leu53. Altogether, the dimer interface comprising the three interlocking helices, buries c.2,600$Å^2$ of its surface.

Interestingly, the lower portions of the crossing helices interact with the LisH domain in a very similar way to the analogous helices in the Lis1 structure. However, in the Lis1 structure one of the helices is bent so as to make the structure asymmetrical (Supplementary Fig. 1b). Instead of the splayed ends of the crossing helices observed in TBL1, the helices in Lis1 form a coiled coil. This appears to be a genuine difference between TBL1 and Lis1 since the asymmetry in Lis1 is observed in two dimers within the crystal lattice. In the case of TBL1 we observe a symmetrical arrangement in the crystals of the long and the short proteins for which the crystal packing environment is quite distinct. There are further notable differences between Lis1 and TBL1 in the path of the loop that joins the four-helix bundle to the additional helices. This makes the shape and character of the TBL1 surface quite distinct from that of Lis1.

In TBL1, the region C-terminal to the LisH motif has been suggested to contain an F-box-like motif [34]. However this region in TBL1 is rather different in both sequence and structure from established F-box motifs and it seems unlikely that it shares the same functionality.

Tetramerization interface

Within the crystal lattice, two TBL1-NTD dimers interact through the base of the four-helix bundle creating a tetramer. Several surface-exposed residues interdigitate at the interface (Fig. 3). His23 makes a hydrogen bond to its symmetry partner across the tetramer interface and also stacks on Phe26 in the other dimer. Ile30 is in non-polar contact with Phe26 and Ile30'. The four Thr27 sidechains in the two dimers are positioned so as to make hydrogen bonds with an ordered water molecule at the centre of the interface (Figs 3c,d). Together

these interactions between TBL1 dimers bury c.1100Å^2. Given the character of the interface, it seems likely that this tetramerization is biologically relevant. This is supported by the finding that the shorter TBL1(1-71) also forms a tetramer in the crystal lattice and a third crystal form of TBL1(1-90), which diffracts to 3.9Å, has three tetramers in the asymmetric unit (Supplementary Fig. 2a). All other packing interactions in these lattices are different. Further support for a biologically relevant tetramer comes from gel filtration analyses, which are consistent with TBL1 being a tetramer in solution (Supplementary Fig. 2b). Furthermore, mutation of Phe26 at the tetramerization interface results in a gel filtration profile consistent with a dimer. Finally NMR HSQC spectra of the wild-type and mutant proteins strongly support the interpretation of tetramers and dimers respectively (Supplementary Fig. 3).

Interestingly the LisH motif containing protein FOP also forms a tetramer in the crystal lattice using the analogous interface. Exposed phenylalanine residues mediate stacking interactions between the two dimers. However it has not been suggested that this is a biologically relevant interface in this protein [39]. Lis1 does not form a tetramer in the crystal lattice [38].

SMRT and GPS2 bind to overlapping surfaces on TBL1

Since both SMRT and GPS2 interact directly with TBL1, we expected TBL1 to have two distinct interaction surfaces. Examination of the surface of the TBL1 dimer reveals a number of candidate interaction surfaces (Fig. 4a,b). One of these (indicated ‘A’) is formed between the helical arms of TBL1 and hence has an internal two-fold symmetry. It consists of fairly wide groove at the base of which lie two tyrosine rings (Tyr59) making a largely non-polar platform. Two other, symmetry related, candidate interaction surfaces are two deep grooves below the helical arms of TBL1 (indicated ‘B’ in figure 4b,c). These grooves are remarkably non-polar in character and are formed from the sidechains of: Ile3, Val8, Phe10, Leu11, Ile39, Leu43, Val44, Pro45, Ala48, Ile52, Leu57’, and Val60’. Glu7 is the only polar residue that contributes to this surface.

To test whether these surfaces on TBL1 are important for interaction with SMRT or GPS2 we made a number of mutations of largely solvent exposed residues that would not be predicted to perturb the global fold of the protein but might perturb intermolecular interactions. The ability of these mutant proteins to bind to SMRT and GPS2 was tested by pull-down assays. No mutations in site ‘A’ were found to perturb interaction with either SMRT or GPS2 (data not shown). However, mutations in three amino acids in site ‘B’ (Ile39, Leu57 and Val60) did result in a significant reduction in the ability of both SMRT and GPS2 to bind to TBL1, but did not affect the behavior of TBL1 suggesting that the domain was still folded correctly. The most marked effect was seen with the mutation V60N which essentially abolished interaction with both proteins (Fig. 4d-f). The finding that SMRT and GPS2 seem to bind to the same surface of TBL1 is at first sight surprising, but makes sense in the context of the whole complex (see below).

To confirm that the V60N mutation prevents co-repressor recruitment in cell-based assays, we exploited the observation that Gal4-DBD fused TBL1-NTD is able to repress transcription of a luciferase reporter gene in a dose-dependent fashion (Fig. 4g). In contrast to repression mediated by the wild-type TBL1-NTD, the V60N mutation does not repress transcription of the reporter gene - presumably since it is unable to recruit the co-repressor complex and associated HDACs (Fig. 4h) .

Identifying a common TBL1 interaction motif in SMRT & GPS2

As mentioned above, the finding that SMRT and GPS2 interact in an antiparallel orientation places the TBL1 interaction regions from both partners at the same end of the coiled-coil.

The further finding that GPS2 and SMRT both interact in the symmetry related non-polar grooves on TBL1 suggested an elegant matching of symmetry such that the two-fold symmetry of the TBL1 homodimer is matched by the anti-parallel orientation of the SMRT–GPS2 heterodimer (Fig. 5a). This prompted us to look for a sequence motif that might be present in both SMRT and GPS2 and at a similar distance from the coiled-coil motif. Figure 5b shows the reverse (antiparallel) alignment of GPS2 and SMRT. Clearly there is no extensive sequence homology between the two proteins. However a short region in both proteins is predicted to have helical secondary structure and there are similarities in the sequence of this region in the two proteins defining a short motif: A-x-x-A/L-H-R/K-x-Φ (where Φ is a large non-polar residue). Importantly this sequence motif is conserved in the SMRT homologue, NCoR, and in all species of SMRT, NCoR and GPS2 that could be identified in the databases. When this motif is plotted as a helical wheel it is clear that it would form a helix with one conserved non-polar surface and a less conserved polar surface but with a conserved basic residue (Fig. 5c).

To test whether this probable amphipathic alpha helix is the region that interacts with TBL1, we mutated three amino acids in the motif (A-x-x-A/L-H-R/K-x-Φ motif to A-x-x-A/L-A-E-x-A). Pull down assays (Fig. 5d) clearly show that in both GPS2 and in SMRT the mutation of these residues totally abolishes interaction with TBL1. This finding was further confirmed using mammalian two-hybrid assays in which mutations in SMRT abolished the ability of VP16-TBL1 to activate a reporter gene (through interaction with Gal-SMRT) and vice versa with the opposite tags (Figs. 5e,f).

To gain an indication of the relative binding affinity of GPS2 and SMRT peptides for TBL1, we performed *in vitro* fluorescence polarization assays with purified proteins (Fig 6a,b). The dissociation constants for the SMRT(227-260) and GPS2(1-52) peptides are 14.7 (s.d. 0.9) μM and 5.1 (s.d. 0.3) μM respectively, suggesting a relatively weak interaction with TBL1. However the coiled-coil interaction between SMRT and GPS2 means that the SMRT–GPS2 complex is likely to interact more tightly with TBL1. To explore this we created a chimeric peptide in which residues 1-49 of GPS2 are fused with residues 220-260 of SMRT (Fig 6a). This peptide bound with an apparent affinity of 0.95 (s.d. 0.1) μM. We would expect that the interaction with the chimeric peptide would mimic the interaction with the SMRT–GPS2 complex. The higher binding affinity emphasizes the importance of the three-way interactions in mediating assembly of the complex.

Confirmation that the interactions seen in the *in vitro* assays are relevant *in vivo* was obtained using co-immunoprecipitation assays in which a Flag-tagged SMRT–GPS2 chimera was transfected and used to co-immunoprecipitate endogenous and co-transfected full-length TBL1 (Fig. 6c-e). A chimeric peptide in which both the TBL1 interaction sites were mutated (see Fig. 5d) was unable to co-immunoprecipitate TBL1. The interaction between the chimera and TBL1 is sufficiently robust such that relatively large amounts of the two proteins can be purified from HEK293 cells as a binary complex (see the coomassie stained gel Fig. 6e).

Further support for the role of the non-polar grooves in the TBL1 tetramer mediating interaction with SMRT and GPS2 was provided in a mammalian two-hybrid experiment in which the TBL1 V60N mutation showed significantly reduced interaction with the SMRT–GPS2 chimera (Fig. 6f).

Modeling the TBL1 interaction with SMRT and GPS2 peptides

To gain insight into the possible modes of interaction of these peptides with TBL1 we used HADDOCK [40] to dock both SMRT and GPS2 peptides into the groove on the surface of TBL1. The constraint on the docking was the identification of a broad surface on TBL1

encompassing the binding groove (identified by mutagenesis). The docking calculations yielded a dominant cluster for both peptides (144 for SMRT and 83 for GPS2, out of 200 solutions). Strikingly these solutions exhibit a common mode of interaction with TBL1 (Fig. 7a-c) that comprises not only a common orientation of the interaction helix but also many common details in the interactions of individual amino acid side chains at the interface. The common residues that define the interaction motif, all make important interactions at the interface. The histidine and non-polar residues are buried at the interface and the basic residue on the back face of the helix interacts with two glutamic acid residues (Glu61 & Glu68) in TBL1. Glu7 is positioned so as to "cap" the SMRT and GPS2 interaction helices, interacting favorably with the helix dipole. Based on these docking solutions it is easy to understand why the respective mutations in TBL1 and SMRT/GPS2 abolish the interaction.

Discussion

Studies from several laboratories have suggested that TBL1 and TBLR1 are core components of the SMRT and NCoR repression complexes [16-18]. This complex serves to recruit and activate the histone deacetylase activity of HDAC3 and thereby plays a key role in the regulated repression of transcription [23,25,41,42]. Here we report the structure of the highly conserved (from yeast to man) amino terminal domain of TBL1 (TBL1-NTD).

We also present a model, based on mapping, pull-down assays, mutagenesis and an NMR structure, of how the SMRT–GPS2 forms a heterodimeric complex and interacts with the TBL1-NTD. It is clear from our findings that the TBL1-NTD plays an important role as a structural scaffold in mediating the assembly of this ternary complex and that the three-way interaction directs a concerted assembly process.

The crystal structure of the TBL1-NTD reveals a tetrameric organization. Dimerization of the TBL1-NTD domain was expected on the basis of comparison with other LisH containing proteins [38,39]. A key difference of the TBL1 dimer from the other LisH proteins, is the positioning of the splayed helical arms creating an extended structure and two interaction grooves. Both of these features appear to be key to the biological function of TBL1 (see below).

We have shown that the binding of SMRT and GPS2 to TBL1 is significantly enhanced as a result of the tight coiled-coil heterodimerization interface between two partners. Furthermore we have demonstrated, using multiple interaction assays, that SMRT and GPS2 interact with TBL1 through a very short helical sequence motif found in both proteins. The identification of this short interaction motif common to SMRT, NCoR and GPS2 raises the strong possibility that other proteins might contain one or two copies of this motif and also recruit TBL1/TBLR1 through interaction with the same surface. This would be analogous to nuclear receptors recruiting multiple LxxLL containing co-activators. Indeed, if this were to be the case, then it could explain why TBL1 and TBLR1 have been reported to be associated with complexes involved in the activation of transcription [29,43].

The finding that TBL1 was a tetramer in the crystal lattice was surprising to us since at no time had we observed two species of TBL1 suggesting a dimer–tetramer exchange. Accordingly it was important to find evidence supporting the biological relevance for the tetramer observed in the crystals. Strong support for a tetramer in solution came from the dramatically altered behavior of the protein (apparent from NMR and gel-filtration studies) following mutation of a key non-polar residue at the tetramer interface (F26A). This unequivocally showed that the wild type protein is a tight non-dissociating tetramer in solution.

Interestingly, the yeast co-repressor protein Sif2p, a homologue of TBL1, has also been reported to form a tetramer through the amino terminal domain [44]. Indeed oligomerization of other WD40-containing co-repressor proteins appears to a common feature including GROUCHO from Drosophila; TUP1 from yeast and the eukaryotic TLE co-repressor proteins [45,46].

Evidence from other laboratories has suggested that the oligomerization mediated by the TBL1-NTD is critical for the biological function of TBL1. Mutations in this region of the protein abolish the repression activity of the protein as well as its interaction with chromatin and other components of the repression machinery [36]. Furthermore it has been suggested that this region of the protein is also required for the nuclear localization of TBL1 and it is proposed that, in general, LisH mutations are likely to be associated with disease [47].

The finding that TBL1 is a tetramer explains many previous observations in the field. First, it explains why the repression complex can contain both TBL1 and TBLR1 since both the dimerization and tetramerization interfaces are absolutely conserved we would expect that the two proteins would assemble to form heterodimers and heterotetramers. The formation of a tetramer would allow two co-repressor proteins to bind to the TBL1 scaffold, suggesting that it might be possible for SMRT and NCoR to be simultaneously associated with the complex. Whilst some gene promoters have been reported to recruit both SMRT and NCoR [48,49] these may exist in separate complexes since CoIP assays suggest that the repression complexes contain one or the other, but not both, of the co-repressors (e.g. [50]). Intriguingly, recent evidence suggests that SMRT is able to form homodimers and heterodimers with NCoR [51]. Such dimers would be ideally suited to interact with a TBL1 tetramer and would readily account for the very large (1-2MDa) size observed for the co-repressor complex when purified from nuclear extracts [16-18].

A model of the core repression complex (based on the available structures of the various components and their homologues is shown in figure 7d. It is intriguing that the nature of the splayed helical arms of TBL1 tetramer positions the four C-terminal WD40 motifs in TBL1 at the ends of helical arms at some distance from each other (c. 22nm). This raises a key issue: what are the functional roles of the WD40 motifs? In general terms WD40 motifs have been found to be versatile protein-protein interaction modules. In some proteins such as WDR5 and p55 it has been found that the WD40 motifs mediate interaction with histone tails [52,53]. Given the established interactions between TBL1 and histones it would seem reasonable to suggest that the WD40 motifs might also mediate interaction with chromatin [24,35,36]. The distance between the WD40 domains would suggest that the complex might be able to associate with adjacent nucleosomes in de-condensed chromatin and thereby effectively target histone deacetylase activity associated with the co-repressor proteins to active chromatin and promote subsequent condensation. Thus TBL1 is likely to serve as a scaffold for a chromatin-targeted machine. Indeed the recent finding that HDAC3 containing complexes are associated with transcriptionally active genes [54] suggests that SMRT/NCoR–TBL1–GPS2 complex may play a role in resetting the chromatin after each round of transcription. This could explain why TBL1 has been reported to be associated with activators of transcription and may serve as an exchange factor through recruitment of the ubiquitination and proteosomal machinery [34].

In conclusion, we report the first structural view of the core SMRT/NCoR repression complex. This reveals the concerted nature of the assembly of the complex and gives insight into the nature and stoichiometry of the chromatin targeted transcriptional repression machinery.

Supplementary Material

Refer to Web version on PubMed Central for supplementary material.

Acknowledgments

We are grateful to Peter Moody, Paul Elliot, and the beamline staff at DIAMOND and ESRF for help with data collection. This work was supported by the Wellcome Trust [085408] and the Medical Research Council.

Appendix

Methods

Protein expression purification and mutagenesis

TBL1 constructs (residues 1-71 and 1-90) were expressed with and without amino-terminal His6 affinity tags using the pETduet vector (Novagen). Fragments of SMRT (residues 167-297, 167-207 and 227-297) and TBL1 were cloned into the pET41a vector for expression with an N-terminal GST tag, followed by a TEV protease cleavage site. The GPS2 fragments (residues 1-90, 1-60 and 53-90) were cloned into the pET13 vector for expression without any affinity tag. Proteins were expressed in BL21 (DE3) cells at 37ºC. Protein expression was induced by addition of 0.4 mM IPTG for 3 hours.

For crystallization experiments, the His6 tagged TBL1 proteins were purified on Nickel NTA agarose (Qiagen) followed by gel filtration chromatography using a Superdex-S200 26/60 column (GE Healthcare). Protein was eluted from the gel filtration column in 100mM NaCl and 50mM Tris-HCl pH7.4 and concentrated in this buffer to 8mg ml-1.

For NMR experiments, the GST tagged SMRT and untagged GPS2 fragment were expressed separately in minimal media with 15N ammonium chloride and 13C glucose. The cell suspension was mixed prior to lysis and the complex purified using Glutathione Sepharose resin. TEV protease was used to remove the GST tag and release the complex from the resin. The complex was further purified by gel filtration (Superdex S200 26/60) and concentrated to 0.4mM in 100mM NaCl and 50mM Tris-HCl pH7.4 and then exchanged into 20mM deuterated Tris-HCl pH7.0 including protease inhibitor (Roche).

Mutations were created by QuikChange (Stratagene) site-directed mutagenesis and mutants proteins were expressed and purified in exactly the same manner as wild type proteins.

GST co-purification / pull-down assays

GST tagged bait proteins and untagged target proteins were expressed separately and cell suspensions mixed before lysis. The cleared supernatants were mixed with Glutathione Sepharose resin (GE Healthcare), washed stringently and the bound proteins were assayed by SDS PAGE. SeeBlue2 molecular weight markers (Invitrogen) were used on all gels.

NMR spectroscopy and structure calculations

NMR spectra were acquired, assigned and structures calculated as described in the Supplementary Methods.

Crystallization and X-ray structure determination

Initial crystal “hits” were obtained from a screen of 1440 conditions using an Innovadyne Screenmaker crystallization robot. Optimized crystals of both TBL1 fragments were grown at room temperature using the vapor diffusion method. 1μl of protein (8 mg ml^{-1}) was mixed with 1μl of reservoir solution which contained 15% (v/v) 2,4-methylpentanediol, 0.05M

Sodium Acetate pH 4.5 for the His6-TBL1(1-71) crystals and 17% (w/v) PEG 4K, 0.2M $MgCl_2$, 0.1M Tris-HCl pH 8.5 for the His6-TBL1(1-90) crystals. Both crystals were cryo-protected by the addition 19% (v/v) methylpentanediol.

Diffraction data from the $P6_122$ and $P2_12_12_1$ crystals of TBL1(1-90) were collected at Diamond I03 and I04 respectively. Data for the $P3_112$ crystals were collected at ESRF ID14.2. Data were processed using mosflm and scala [55,56]. The structure was solved for the $P6_122$ crystals by molecular replacement using Phaser [57] with a 30% model based on the four-helix bundle dimerization domain from the Lis1 protein (aa 9-36; pdbcode 1UUJ). Initially electron density consistent with the TBL1 sequence was observed, but with no additional density beyond the model. The additional TBL1 sequence was fitted following multiple rounds of refinement and building using Refmac, CNS, and Coot[58-60]. The final model contains amino-acids 2-75 chain A and 2-36 and 40-66 chain B. This model was used to solve the structure in the $P3_212$ and $P2_12_12_1$ crystals. Due to the low resolution of data for these crystals only limited refinement was performed in atomic positions and grouped B-factors in Refmac and CNS respectively.

Fluorescence polarization assays

Fluorescence polarization assays were performed and analyzed as described in the Supplementary Methods.

Transient transfection, reporter gene and co-immunoprecipitation assays

The various constructs: MH-100-TK-Luc reporter gene (containing Gal binding sites), pCMX β gal along with VP16-fused TBL1(1-90) and GAL-DBD-fused SMRT(227-251) or GAL-DBD-fused SMRT(227-251 AEA mutant) were transfected into 293T cells using jetPEI reagent (Qbiogene) according to the manufacturer's instructions. Cells were lysed and assayed for reporter expression 48hr after transfection.

Luciferase activity was determined using the Luciferase Assay System (Promega), and normalized to the β-galactosidase activity. Measurements were carried out using a Wallac Victor 2 multilabel counter. All experiments were done in triplicate.

For the co-immunoprecipitation assays, full length TBL1, chimera GPS2(1-49)–SMRT(220-260) and chimera GPS2(1-49)–SMRT(220-260) AEA double mutant were cloned into the pcDNA3 vector, the chimera constructs contained a N-terminal His10-FLAG3 tag. Constructs were transfected/co-transfected into 293T cells using jetPEI reagent (Qbiogene). Cells were lysed after 48hrs and proteins were immunoprecipitated using anti-Flag M1 agarose affinity gel (Sigma) in accordance with the manufacturer's instructions. Proteins were analyzed by SDS-PAGE followed by Western blotting using antibodies to TBL1 (Abcam) or the FLAG tag (Sigma).

Modeling TBL1-peptide interactions

The interaction between TBL1 and the SMRT/GPS2/NCoR peptides was modeled using protein-protein docking within HADDOCK [40]. Residues lining the elongated binding pocket of TBL1 were selected as active site for docking as well as all residues of the SMRT and GPS2 peptides, which were initially built as helices.

The default HADDOCK docking and refinement protocol generates 1,000 independent rigid-body minimizations and docked complexes. The 200 lowest-intermolecular energy solutions were subjected to semi-flexible simulated annealing, wherein side chain flexibility was permitted for the active site residues. Subsequently each structure was refined in explicit water and subjected to cluster analysis.

The refined protein complexes were grouped into clusters using a 2Å threshold r.m.s. deviation. Ten complexes from each cluster with the lowest overall energy were subjected to rational analysis.

References

1. Lazar MA. Nuclear receptor corepressors. Nuclear receptor signaling. 2003; 1:e001. [PubMed: 16604174]
2. Ahmad KF, et al. Mechanism of SMRT corepressor recruitment by the BCL6 BTB domain. Mol Cell. 2003; 12:1551–1564. [PubMed: 14690607]
3. Gelmetti V, et al. Aberrant recruitment of the nuclear receptor corepressor-histone deacetylase complex by the acute myeloid leukemia fusion partner ETO. Mol Cell Biol. 1998; 18:7185–7191. [PubMed: 9819405]
4. Jayne S, Zwartjes CG, van Schaik FM, Timmers HT. Involvement of the SMRT/NCoR-HDAC3 complex in transcriptional repression by the CNOT2 subunit of the human Ccr4-Not complex. Biochem J. 2006; 398:461–467. [PubMed: 16712523]
5. Kao HY, et al. A histone deacetylase corepressor complex regulates the Notch signal transduction pathway. Genes Dev. 1998; 12:2269–2277. [PubMed: 9694793]
6. Wu X, Li H, Park EJ, Chen JD. SMRTE inhibits MEF2C transcriptional activation by targeting HDAC4 and 5 to nuclear domains. J Biol Chem. 2001; 276:24177–24185. [PubMed: 11304536]
7. Yoon HG, Chan DW, Reynolds AB, Qin J, Wong J. N-CoR mediates DNA methylation-dependent repression through a methyl CpG binding protein Kaiso. Mol Cell. 2003; 12:723–734. [PubMed: 14527417]
8. Lutterbach B, et al. ETO, a target of t(8;21) in acute leukemia, interacts with the N-CoR and mSin3 corepressors. Mol Cell Biol. 1998; 18:7176–7184. [PubMed: 9819404]
9. Jepsen K, et al. Combinatorial roles of the nuclear receptor corepressor in transcription and development. Cell. 2000; 102:753–763. [PubMed: 11030619]
10. Jepsen K, et al. SMRT-mediated repression of an H3K27 demethylase in progression from neural stem cell to neuron. Nature. 2007; 450:415–419. [PubMed: 17928865]
11. Barroso I, et al. Dominant negative mutations in human PPARgamma associated with severe insulin resistance. Nature. 1999; 402:880–883. [PubMed: 10622252]
12. Cheng GX, et al. Distinct leukemia phenotypes in transgenic mice and different corepressor interactions generated by promyelocytic leukemia variant fusion genes PLZF-RARalpha and NPM-RARalpha. Proc Natl Acad Sci USA. 1999; 96:6318–6323. [PubMed: 10339585]
13. Hong SH, David G, Wong CW, Dejean A, Privalsky ML. SMRT corepressor interacts with PLZF and with the PML-retinoic acid receptor alpha (RARalpha) and PLZF-RARalpha oncoproteins associated with acute promyelocytic leukemia. Proc Natl Acad Sci USA. 1997; 94:9028–9033. [PubMed: 9256429]
14. Melnick AM, et al. The ETO protein disrupted in t(8;21)-associated acute myeloid leukemia is a corepressor for the promyelocytic leukemia zinc finger protein. Mol Cell Biol. 2000; 20:2075–2086. [PubMed: 10688654]
15. Picard F, et al. Sirt1 promotes fat mobilization in white adipocytes by repressing PPAR-gamma. Nature. 2004; 429:771–776. [PubMed: 15175761]
16. Guenther MG, et al. A core SMRT corepressor complex containing HDAC3 and TBL1, a WD40-repeat protein linked to deafness. Genes Dev. 2000; 14:1048–1057. [PubMed: 10809664]
17. Li J, et al. Both corepressor proteins SMRT and N-CoR exist in large protein complexes containing HDAC3. EMBO J. 2000; 19:4342–4350. [PubMed: 10944117]
18. Wen YD, et al. The histone deacetylase-3 complex contains nuclear receptor corepressors. Proc Natl Acad Sci USA. 2000; 97:7202–7207. [PubMed: 10860984]
19. Heinzel T, et al. A complex containing N-CoR, mSin3 and histone deacetylase mediates transcriptional repression. Nature. 1997; 387:43–48. [PubMed: 9139820]
20. Nagy L, et al. Nuclear receptor repression mediated by a complex containing SMRT, mSin3A, and histone deacetylase. Cell. 1997; 89:373–380. [PubMed: 9150137]

21. Ishizuka T, Lazar MA. The nuclear receptor corepressor deacetylase activating domain is essential for repression by thyroid hormone receptor. Mol Endocrinol. 2005; 19:1443–1451. [PubMed: 15695367]
22. Yin L, et al. Rev-erb{alpha}, a Heme Sensor That Coordinates Metabolic and Circadian Pathways. Science. 2007 [PubMed: 18006707]
23. Guenther MG, Barak O, Lazar MA. The SMRT and N-CoR corepressors are activating cofactors for histone deacetylase 3. Mol Cell Biol. 2001; 21:6091–6101. [PubMed: 11509652]
24. Yoon HG, et al. Purification and functional characterization of the human N-CoR complex: the roles of HDAC3, TBL1 and TBLR1. EMBO J. 2003; 22:1336–1346. [PubMed: 12628926]
25. Zhang J, Kalkum M, Chait BT, Roeder RG. The N-CoR-HDAC3 nuclear receptor corepressor complex inhibits the JNK pathway through the integral subunit GPS2. Mol Cell. 2002; 9:611–623. [PubMed: 11931768]
26. Hörlein AJ, et al. Ligand-independent repression by the thyroid hormone receptor mediated by a nuclear receptor co-repressor. Nature. 1995; 377:397–404. [PubMed: 7566114]
27. Peng YC, Breiding DE, Sverdrup F, Richard J, Androphy EJ. AMF-1/Gps2 binds p300 and enhances its interaction with papillomavirus E2 proteins. J Virol. 2000; 74:5872–5879. [PubMed: 10846067]
28. Peng YC, et al. AMF1 (GPS2) modulates p53 transactivation. Mol Cell Biol. 2001; 21:5913–5924. [PubMed: 11486030]
29. Jakobsson T, et al. GPS2 is required for cholesterol efflux by triggering histone demethylation, LXR recruitment, and coregulator assembly at the ABCG1 locus. Mol Cell. 2009; 34:510–518. [PubMed: 19481530]
30. Zhang D, Harry GJ, Blackshear PJ, Zeldin DC. G-protein pathway suppressor 2 (GPS2) interacts with the regulatory factor X4 variant 3 (RFX4_v3) and functions as a transcriptional co-activator. J Biol Chem. 2008; 283:8580–8590. [PubMed: 18218630]
31. Degenhardt YY, Silverstein SJ. Gps2, a protein partner for human papillomavirus E6 proteins. J Virol. 2001; 75:151–160. [PubMed: 11119584]
32. Lee TH, Yi W, Griswold MD, Zhu F, Her C. Formation of hMSH4-hMSH5 heterocomplex is a prerequisite for subsequent GPS2 recruitment. DNA Repair (Amst). 2006; 5:32–42. [PubMed: 16122992]
33. Yan HT, et al. Molecular analysis of TBL1Y, a Y-linked homologue of TBL1X related with X-linked late-onset sensorineural deafness. J Hum Genet. 2005; 50:175–181. [PubMed: 15834507]
34. Perissi V, Aggarwal A, Glass CK, Rose DW, Rosenfeld MG. A corepressor/coactivator exchange complex required for transcriptional activation by nuclear receptors and other regulated transcription factors. Cell. 2004; 116:511–526. [PubMed: 14980219]
35. Hartman HB, Yu J, Alenghat T, Ishizuka T, Lazar MA. The histone-binding code of nuclear receptor co-repressors matches the substrate specificity of histone deacetylase 3. EMBO Rep. 2005; 6:445–451. [PubMed: 15832170]
36. Choi HK, et al. Function of Multiple LisH/WD-40 Repeat-Containing Proteins in Feed-Forward Transcriptional Repression by SMRT/N-CoR Corepressor Complexes. Mol Endocrinol. 2008 [PubMed: 18202150]
37. Oakley MG, Hollenbeck JJ. The design of antiparallel coiled coils. Curr Opin Struct Biol. 2001; 11:450–457. [PubMed: 11495738]
38. Kim MH, et al. The structure of the N-terminal domain of the product of the lissencephaly gene Lis1 and its functional implications. Structure. 2004; 12:987–998. [PubMed: 15274919]
39. Mikolajka A, et al. Structure of the N-terminal domain of the FOP (FGFR1OP) protein and implications for its dimerization and centrosomal localization. J Mol Biol. 2006; 359:863–875. [PubMed: 16690081]
40. Dominguez C, Boelens R, Bonvin AM. HADDOCK: a protein-protein docking approach based on biochemical or biophysical information. J Am Chem Soc. 2003; 125:1731–1737. [PubMed: 12580598]
41. Codina A, et al. Structural insights into the interaction and activation of histone deacetylase 3 by nuclear receptor corepressors. Proc Natl Acad Sci USA. 2005; 102:6009–6014. [PubMed: 15837933]

42. Li J, Lin Q, Wang W, Wade P, Wong J. Specific targeting and constitutive association of histone deacetylase complexes during transcriptional repression. Genes Dev. 2002; 16:687–692. [PubMed: 11914274]
43. Li J, Wang CY. TBL1-TBLR1 and beta-catenin recruit each other to Wnt target-gene promoter for transcription activation and oncogenesis. Nat Cell Biol. 2008; 10:160–169. [PubMed: 18193033]
44. Cerna D, Wilson DK. The structure of Sif2p, a WD repeat protein functioning in the SET3 corepressor complex. J Mol Biol. 2005; 351:923–935. [PubMed: 16051270]
45. Chen G, Courey AJ. Groucho/TLE family proteins and transcriptional repression. Gene. 2000; 249:1–16. [PubMed: 10831834]
46. Varanasi US, Klis M, Mikesell PB, Trumbly RJ. The Cyc8 (Ssn6)-Tup1 corepressor complex is composed of one Cyc8 and four Tup1 subunits. Mol Cell Biol. 1996; 16:6707–6714. [PubMed: 8943325]
47. Gerlitz G, Darhin E, Giorgio G, Franco B, Reiner O. Novel functional features of the Lis-H domain: role in protein dimerization, half-life and cellular localization. Cell Cycle. 2005; 4:1632–1640. [PubMed: 16258276]
48. Ghisletti S, et al. Cooperative NCoR/SMRT interactions establish a corepressor-based strategy for integration of inflammatory and anti-inflammatory signaling pathways. Genes Dev. 2009; 23:681–693. [PubMed: 19299558]
49. Hong W, et al. Bag-1M inhibits the transactivation of the glucocorticoid receptor via recruitment of corepressors. FEBS Letters. 2009; 583:2451–2456. [PubMed: 19595997]
50. Tomita A, Buchholz DR, Shi YB. Recruitment of N-CoR/SMRT-TBLR1 corepressor complex by unliganded thyroid hormone receptor for gene repression during frog development. Mol Cell Biol. 2004; 24:3337–3346. [PubMed: 15060155]
51. Varlakhanova N, Hahm JB, Privalsky ML. Regulation of SMRT corepressor dimerization and composition by MAP kinase phosphorylation. Mol Cell Endocrinol. 2010
52. Couture JF, Collazo E, Trievel RC. Molecular recognition of histone H3 by the WD40 protein WDR5. Nat Struct Mol Biol. 2006; 13:698–703. [PubMed: 16829960]
53. Song JJ, Garlick JD, Kingston RE. Structural basis of histone H4 recognition by p55. Genes Dev. 2008; 22:1313–1318. [PubMed: 18443147]
54. Wang Z, et al. Genome-wide Mapping of HATs and HDACs Reveals Distinct Functions in Active and Inactive Genes. Cell. 2009; 138:1019–1031. [PubMed: 19698979]
55. Leslie AG. The integration of macromolecular diffraction data. Acta Crystallogr D Biol Crystallogr. 2006; 62:48–57. [PubMed: 16369093]
56. Collaborative Computational Project, N. The CCP4 suite: programs for protein crystallography. Acta Crystallogr D Biol Crystallogr. 1994; 50:760–763. [PubMed: 15299374]
57. McCoy AJ, et al. Phaser crystallographic software. J Appl Crystallogr. 2007; 40:658–674. [PubMed: 19461840]
58. Brunger AT. Version 1.2 of the Crystallography and NMR system. Nat Protoc. 2007; 2:2728–2733. [PubMed: 18007608]
59. Emsley P, Cowtan K. Coot: model-building tools for molecular graphics. Acta Crystallogr D Biol Crystallogr. 2004; 60:2126–2132. [PubMed: 15572765]
60. Murshudov GN, Vagin AA, Dodson EJ. Refinement of macromolecular structures by the maximum-likelihood method. Acta Crystallogr D Biol Crystallogr. 1997; 53:240–255. [PubMed: 15299926]

Europe PMC Funders Author Manuscripts

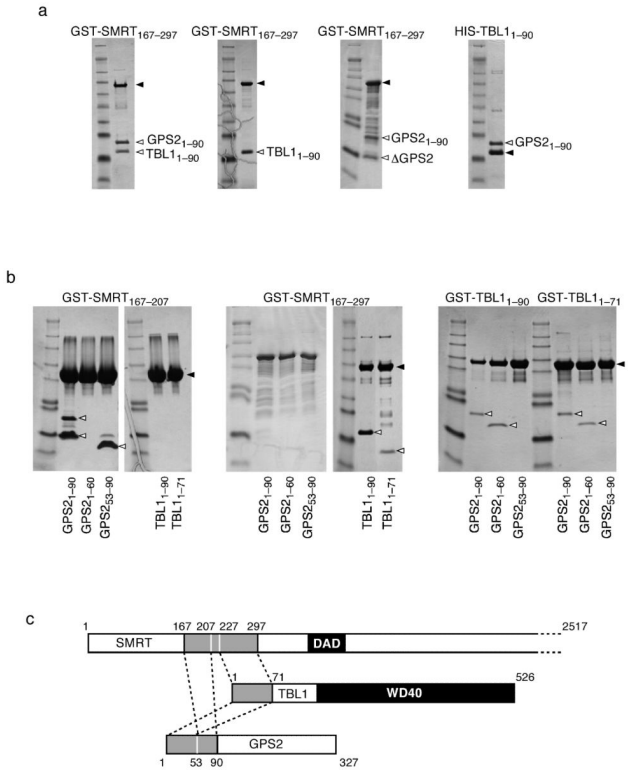

Figure 1.

Mapping the interactions between TBL1, SMRT and GPS2. Panels (a) and (b) show coomassie stained SDS-PAGE gels assaying the interaction between the indicated proteins. (a) The first panel shows co-purification of a ternary complex between GST-SMRT(167-297), TBL1(1-90) and GPS2(1-90). The second, third and fourth panels show co-purification of binary complexes between GST-SMRT(167-297) with TBL1(1-90); GST-SMRT(167-297) with GPS2(1-90) and His-TBL1(1-90) with GPS2(1-90). Note that filled triangles indicate the tagged protein. Both SMRT and GPS2 undergo proteolysis in the absence of TBL1 (ΔGPS2 indicates a degradation product - confirmed by mass spectrometry). (b) Refinement of interaction regions. The tagged protein is listed above the gel and indicated by a filled arrow. Open arrows indicate co-purified interacting proteins. SMRT(167-207) is sufficient for interaction with GPS2(53-90) but does not interact with TBL1. SMRT(227-297) is sufficient for interaction with TBL1(1-71) but not GPS2. TBL1(1-71) is sufficient for interaction with GPS2(1-60) but not GPS2(53-90). In the first panel GPS2(1-90) runs as two species (one is a degradation product - confirmed by mass spectrometry). (c) Schematic representation of the three-way complex.

Europe PMC Funders Author Manuscripts

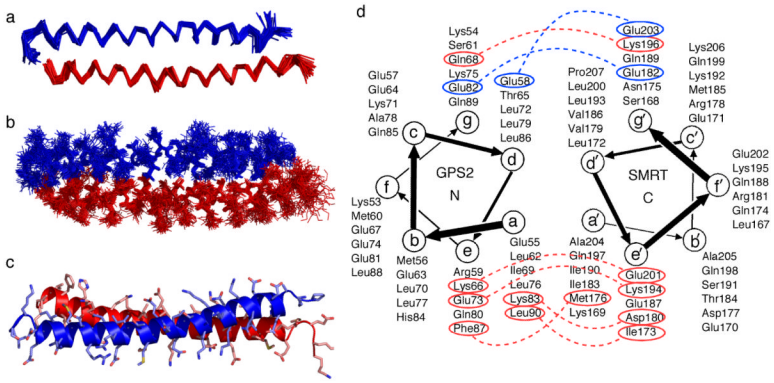

Figure 2.

NMR solution structure of the anti-parallel coiled coil formed by the interaction of SMRT and GPS2. (a) Backbone Cα and (b) all heavy atom superposition of the 10 NMR structures with the fewest NOE violations. SMRT is shown in blue and GPS2 in red. (c) Cartoon representation of the anti-parallel coiled coil structure of SMRT(167-207), and GPS2(53-90). (d) Helical wheel representation to illustrate the amino-acid interactions between SMRT and GPS2 that determine the anti-parallel orientation of the coiled coil. Red lines indicate favorable interactions, blue lines indicate proximity of residues of the same charge (acidic) which appears to be compensated by adjacent basic residues.

Europe PMC Funders Author Manuscripts

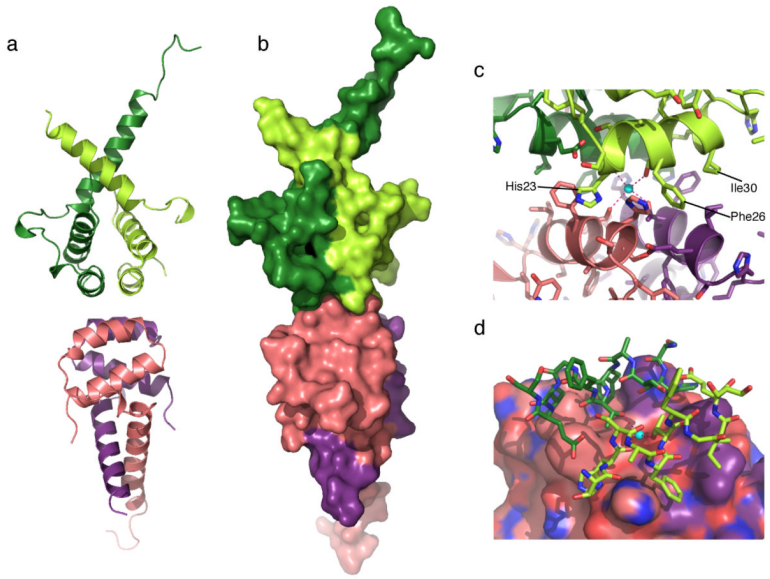

Figure 3.
Crystal structure of the TBL1-NTD tetramer. (a) and (b) Cartoon and surface representations of the overall structure of the TBL1 tetramer. The two homodimers are shown in light/dark green and pink/purple. (c) and (d) Residues involved in the tetramerization of TBL1.

Europe PMC Funders Author Manuscripts

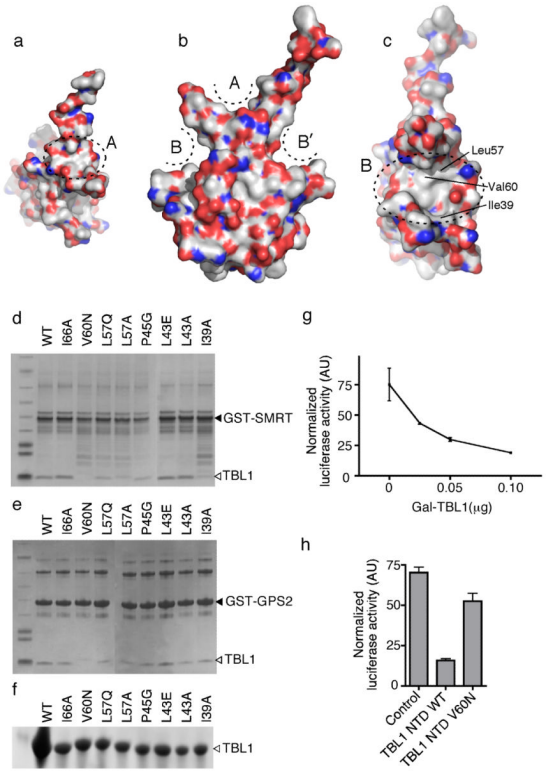

Figure 4.

Binding of SMRT and GSP2 to TBL1. (a), (b), and (c) Surface representations in three different orientations of TBL1 showing two distinct non-polar grooves (indicated A and B) which are potential protein-protein interaction sites. (d) and (e) A number of mutations were made in sites A and B of TBL1 and these mutant proteins (indicated by an open triangle) were tested for their ability to bind to GST-SMRT(227-297) and GST-GPS2(1-60) in co-purification assays (shown by filled triangles). Mutations in Leu57, Val90 and Ile39 caused a significant reduction in the binding of both SMRT (d) and GPS2 (e) to TBL1, suggesting that SMRT and GPS2 interact with the same surface of TBL1. (f) Control for panels (d) and (e) indicating equal expression of the TBL1 mutant proteins. (g) and (h) Mammalian one-hybrid assay showing that Gal-TBL1 causes dose-dependent repression of a Gal-UAS driven reporter gene (luciferase). The V60N mutation in Gal-TBL1 greatly diminishes the repression activity.

Europe PMC Funders Author Manuscripts

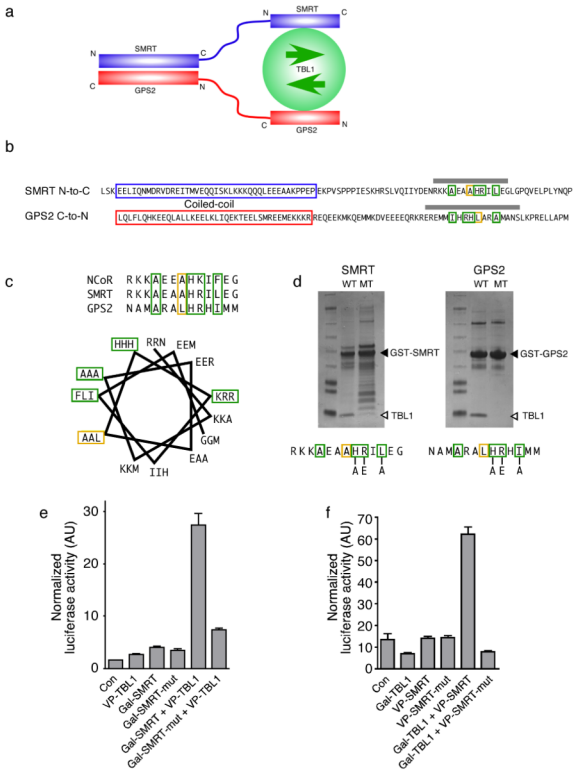

Figure 5.

Identification of a common TBL1 interaction motif in SMRT and GPS2. (a) Schematic showing how the anti-parallel orientation of the coiled-coil positions the TBL1 interaction motifs in SMRT and GPS2 at one end of the coiled coil, such that there is a symmetry match between the SMRT–GPS2 heterodimer and the TBL1 homodimer. (b) An anti-parallel sequence alignment of SMRT and GPS2 based on the anti-parallel coiled coil interaction between SMRT(167-207) and GPS2(53-90). The amino-acids in the NMR structure are outlined in blue and red. A short predicted helical structure for both SMRT and GPS2 at a similar distance from the coiled-coil (indicated by the grey bar above the sequence). A short sequence motif found in both SMRT and GPS2 in this helical region is outlined in green and yellow. (c) Sequence alignment of NCoR, SMRT, and GPS2 showing the important conservation of this motif between the three proteins and a helical wheel representation of these residues showing the arrangement of the conserved, non-polar residues on one side of the helix. (d) Three conserved residues in the motif were mutated both in GST-SMRT(227-297; H242A, R243E, L245A) and GST-GPS2(1-60; H19A, R20E, I22A). These triple mutant proteins were tested for their ability to bind to TBL1(1-90), using a pull down assay. Both mutant proteins fail to bind TBL1. (e & f) The SMRT–TBL1 interaction was tested in a mammalian two hybrid assay with a luciferase reporter. This shows a reciprocal interaction between SMRT and TBL1 in HEK293T cells and that the SMRT AEA mutation abolishes the interaction. Data are shown as mean and s.d.

Europe PMC Funders Author Manuscripts

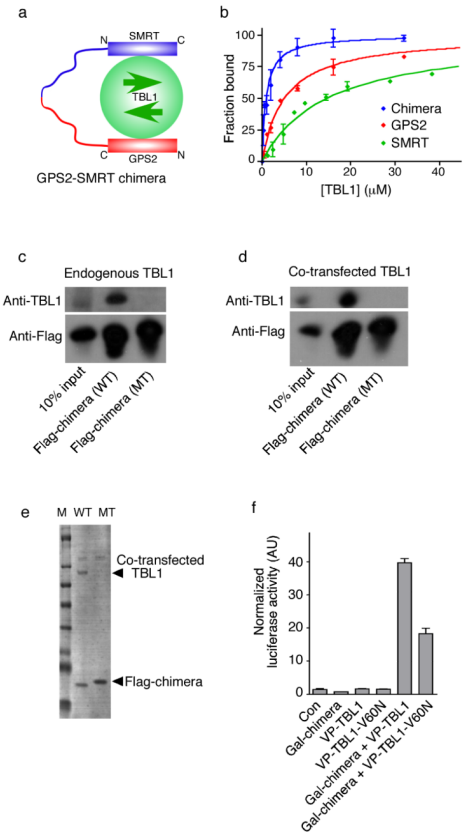

Figure 6.

Interaction of a GPS2–SMRT chimera with TBL1 *in vitro* and *in vivo*. (a) Schematic showing the GPS2–SMRT chimera used for the fluorescence polarization, co-IP and two-hybrid assays (panels b-f). (b) Fluorescence polarization assay of the binding of BODIPY labeled SMRT(227-260), GPS2(1-52) and a chimeric GPS2(1-49)–SMRT(220-260) to His6 TBL1(1-90). The binding curves were analyzed using GraphPad Prism. Dissociation constants are 14.7 μM (s.d. 0.9), 5.1 μM (s.d. 0.3) and 0.95 μM (s.d. 0.1) for the respective proteins. (c), (d) and (e) Co-immunoprecipitation of Flag-tagged GPS2(1-49)–SMRT(220-260) wild-type (WT) and double AEA mutant (MT) chimera with endogenous and co-transfected full-length TBL1. The AEA double mutation in the chimera abolishes interaction with TBL1. In panels (c) and (d) Western blots were probed with antibodies as indicated. Panel (e) shows a coomassie stained gel demonstrating the high purity and yield of the complex. (f) Mammalian two-hybrid assay showing that the interaction of VP-TBL1 with the Gal-fused chimera is significantly reduced (and hence reduced luciferase activity) by the V60N mutation in TBL1. Data are shown as mean and s.d.

Europe PMC Funders Author Manuscripts

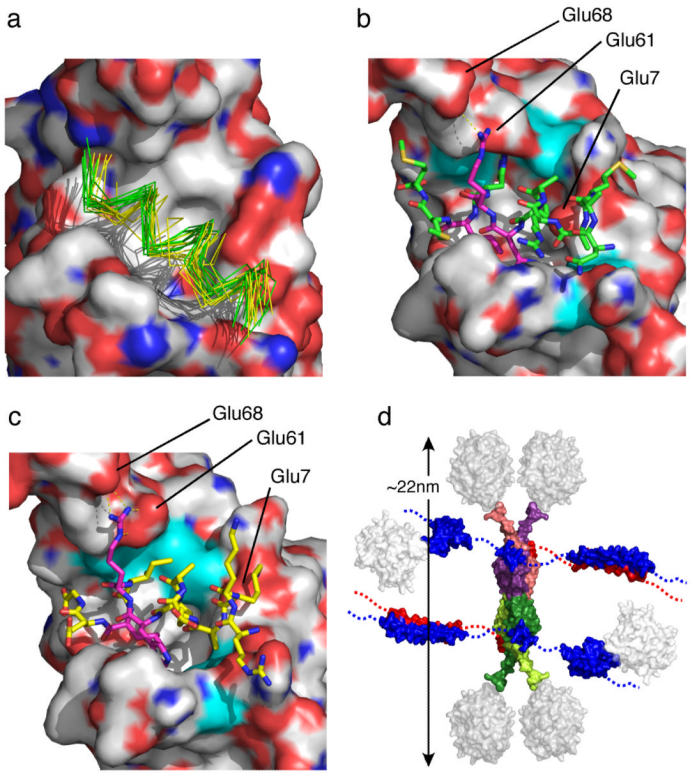

Figure 7.

In silico docking of the SMRT and GPS2 peptides with TBL1 and assembly of the core SMRT/NCoR repression complex. (a-c) Results of the HADDOCK docking of the SMRT and GPS2 peptides into the interaction grooves of TBL1. (a) The 10 lowest-energy docking solutions in the dominant clusters for SMRT (yellow) and GPS2 (green) in the interaction groove of TBL1 (surface representation). These solutions are very similar despite the different sequences of SMRT and GPS2. Panels (b) and (c) show details of the side chain interactions for GPS2 and SMRT respectively. Key residues in TBL1 and SMRT/GPS2, identified by mutagenesis, are colored cyan and magenta respectively. (d) Summary of the structural information available for the assembly of the core SMRT/NCoR repression complex. The TBL1 NTD tetramer is shown in light/dark green and salmon/violet in the centre of the figure. The coiled-coil and TBL1 interacting regions from SMRT and GPS2 are shown in blue and red respectively. The DAD domain from SMRT (pdbcode 1xc5) is also shown in blue. To give an indication of the size of the core complex, WD40 domains (pdbcode 2h9m) and an HDAC catalytic domain (pdbcode 3hgq) are positioned at the C-termini of the TBL1 NTDs and adjacent to the SMRT DAD domain respectively and shown in light grey.

Europe PMC Funders Author Manuscripts

Table 1

NMR structure determination statistics

	Protein
NMR distance and dihedral constraints	
Distance constraints	
Total NOE	808
Intra-residue	177
Inter-residue	
Sequential (|*i* − *j*| = 1)	167
Medium-range (2 <= |*i* − *j*| <= 4)	325
Long-range intrachain (|*i* − *j*| >= 5)	4
Interchain	135
Hydrogen bonds	-
Total dihedral angle restraints	
Φ	-
Ψ	-
Structure statistics	
Violations (mean and s.d.)	
Distance constraints (Å)	0.077 ± 0.033
Dihedral angle constraints (°)	-
Max. distance constraint violation (Å)	0.203
Max. dihedral angle violation (°)	-
Deviations from idealized geometry	
Bond lengths (Å)	0.0021
Bond angles (°)	0.489
Impropers (°)	0.348
Average pairwise r.m.s. deviation ** (Å)	
Well-ordered residues (59-87 GPS2; 174-203 SMRT)	
Heavy	1.11 ± 0.17
Backbone	0.59 ± 0.21
All residues (53-90 GPS2; 166-207 SMRT)	
Heavy	1.64 ± 0.29
Backbone	1.19 ± 0.34

** Pairwise r.m.s. deviation was calculated among 35 refined structures selected from an ensemble of 50.

Table 2

Data collection and refinement statistics (molecular replacement)

	TBL1(1–90)	TBL1(1–71)	TBL1(1–90)
Data collection			
Space group	$P6_122$	$P3_212$	$P2_12_12_1$
Cell dimensions			
a, b, c (Å)	59.54, 59.54, 193.88	47.89, 47.89, 153.81	88.02, 150.19, 164.83
α, β, γ (°)	90, 90,120	90, 90, 120	90, 90, 90
Resolution (Å)	96.22–2.2(2.32–2.2)	76.92–3.2(3.37–3.2)	111.11–3.90 (4.11–3.90)
R_{sym} or R_{merge}	7.3(39.7)	6.2(43.1)	10.7 (31.5)
$I / \sigma I$	15.1(3.9)	20.2(5.1)	9.1 (4.0)
Completeness (%)	99.9(100.0)	99.8(100.0)	99.9 (100)
Redundancy	6.5(6.7)	6.7(6.8)	3.5 (3.6)
Refinement			
Resolution (Å)	51.57–2.2	51.27–3.2	111.11–3.9
No. reflections	10313	3503	19503
R_{work} / R_{free}	23.9/26.7	26.3/31.2	26.9/29.8
No. atoms			
Protein	1041	1014	6228
Ligand/ion			
Water	42	0	0
B-factors	39.69	106.1	101.0
R.m.s. deviations			
Bond lengths (Å)	0.012	0.029	0.011
Bond angles (°)	1.631	2.0	1.238